Article

Photovoltaic System Equipped with Digital Command Control and Acquisition

Med Faysal Yaden, Mustapha Melhaoui, Rajae Gaamouche, Kamal Hirech, Elhadi Baghaz and Khalil Kassmi *

LETAS, Department of Physics, Faculty of Science, University Mohamed the First, Oujda 60000, Morocco; E-Mails: y.faysal@hotmail.fr (M.F.Y.); mustapha_melhaoui@hotmail.com (M.M.); raja.escom@gmail.com (R.G.); hirech@gmail.com (K.H.); e.baghaz@yahoo.fr (E.B.)

* Author to whom correspondence should be addressed; E-Mail: khkassmi@yahoo.fr; Tel.: +212-5-3650-0601/02; Fax: +212-5-3650-0603.

Abstract: In this paper, we present results concerning the design, the realization and the characterization of a photovoltaic system (PV), equipped with a digital controls: Power Point Tracking (MPPT), charge/discharge lead acid batteries, sun tracker and supervision. These different functions are performed with a microcontroller that has capabilities and functions to the reliability of PV systems (signal generation Pulses Width Modulation (PWM), speed *etc*.). Concerning the MPPT control operation, we improved the accuracy and reliability of research by improving the search algorithm "Hill Climbing" taking into account the optimal operation of PV panels depending on weather conditions (temperature and light).The experiment of each block shows that the MPPT control converges instantly the operating point of the PV panels around the maximum power point, independently of sudden changes of the illumination or the load. The control blocks charge/discharge battery and sun tracking show good control of charge/discharge lead acid batteries and the need of sun tracker to increase the power supplied by the PV panel. By using the improved MPPT control, loss of power supplied by the PV panels are very low (below 5%).

Nomenclature

V_{PV}	Photovoltaic voltage (V)
V_s	Output voltage (V)
V_{bat}	Voltage of battery (V)
V_r	Voltage of regulation (V)
V_d	Voltage limit of discharge (V)
I_{PV}	Photovoltaic current (A)
I_S	Output current (A)
I_{bat}	Current of charge of battery (A)
P_{PV}	Photovoltaic power (W)
P_s	Output power (W)
α	Duty cycle
PIC	Programmable Interface Controller
V_1	Terminal voltage of the LDR sensor 1
V_2	Terminal voltage of the LDR sensor 2
V_3	Terminal voltage of the LDR sensor 3
V_4	Terminal voltage of the LDR sensor 4

1. Introduction

The renewable energy revolution is put forward as a solution to our problems of electrical energy production; one such renewable energy source is via photovoltaic (PV) technology, based on the conversion of sunlight into electricity using PV cells [1]. Currently, much research is being carried out on cells (or panels) and on PV systems that exploit this energy [2,3]. Concerning PV systems, the difficulties are the optimization of the power provided by PV panels, its transfer to the load (in our case Battery), good control of charge/discharge lead acid batteries and solar tracking PV panels [2,3]. The discrete blocks of regulation and control suggested are not reliable and induce power losses provided by PV panels [2–4], divergence of PV system [2–4], poor control of the charge/discharge batteries [5] and the collecting of illumination [6,7]. In the majority of PV systems, the major problem is the loss of power supplied by the PV panels because of inaccurate desired maximum power point (MPP) [8,9].

In this regard, we are carrying out research on PV systems; precisely control and regulation blocks [8]. The main objective is to propose a simple technique to implement integrated systems in the same case using a microcontroller with various modules, such as CAN, USART and PWM, to manage the three blocks (MPPT control, controller of charge/discharge batteries and solar tracking).This implementation provides valuable benefits for improving the reliability of energy systems, especially in the field of renewable energy. In the case of the MPPT functioning control, we propose to improve the accuracy and speed of the research of MPP using the results of the optimal functioning of PV [10].

This method also allows removing the perturbation of researching PPM when the power-voltage characteristics of PV panels have several maximum follow on effects of shading [11] or disequilibrium of PV cells [12].

In our study, the microcontroller can perform the following tasks:

- Acquisition and supervision system, which allows the capture of the various electric quantities of the system (currents, voltages, powers, outputs, *etc.*), and projects them on a computer screen.
- Digital MPPT control whose proposed algorithm takes into account the divergence of the system after sudden changes of illumination or load.
- Charge/discharge regulation by ensuring the optimal charge and the good control state of batteries.
- Sun tracking using several techniques, fixed by the supervision system and allowing PV panels to receive maximum energy at every moment of the day.

In this paper, we present the description of the system design and different simulated and experimental results of various blocks.

2. Photovoltaic System Design

2.1. Synoptic Diagram of the System

The overview diagram of the global system designed in this work is shown in Figure 1. The diagram illustrates the blocks:

- The purpose of acquisition and supervision system is to create links to communicate between the different blocks of the global system and send the various electrical values to the computer.
- Digital MPPT controller allows the operating point of the PV panels to converge instantly to the maximum power point (MPP) [2,4].
- The system of the charge/discharge control leads acid batteries. It has the task of managing the charge/discharge process and controls the state of batteries as well.
- The sun tracking has the objective of exposing the PV panel to a maximum degree of irradiation throughout the day by following algorithms and techniques regulated by the monitoring system.

Figure 1. Synoptic diagram of the photovoltaic system.
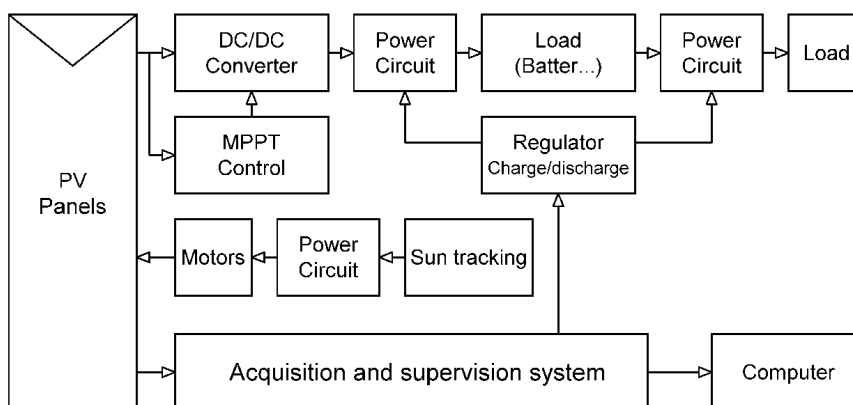
2.2. Digital MPPT Control

The PV system with the MPPT control is shown in Figure 2. This block is used to control the switch of DC-DC converter by generating a PWM signal, its duty cycle is set by the microcontroller (PIC 16F877) depending on irradiance and load variations [2,3]. This microcontroller allows us to

create reliable PV system operations, and has different PORT allowing for more functions, such as: providing an analog input acquisition, sending data to a computer hard disk, visualizing data on a computer screen, and most importantly, implementing all of the subsystem described above in one block.

This block is composed of:

- A voltage divider (R_1, R_2) for the acquisition of the input voltage of the PV generator.
- A shunt resistance (R_{sh}), to take the image of the input current of the PV panels, amplified by an inverting amplifier.
- A microcontroller whose function is to generate a PWM signal, amplified by an amplifier.
- A driver that improves the shape of the signal supplied by the amplifier to have a rectangular signal PWM.

The algorithm of Figure 3 performs the regulation of the power supplied by the PV modules. "Hill Climbing" [13] is the method used in this command which is based on the relation between the power panel and the value of the duty cycle applied to the DC-DC converter. To improve the accuracy and speed of the MPP sought, we added to the algorithm the possibility to search around the MPP. In previous studies, we have studied and modeled the MPP for a given technology depending on the illumination and temperature (Figure 3). We have shown that this varies from 12 V to 16 V when the illumination varies from 200 W/m^2 to 1200 W/m^2 and the temperature varies from 0 to 40 °C. This new research method prevents problems from inaccuracies in the research when the electrical characteristics of PV panels have more maximum power [14] (shading imbalance PV cells, *etc*.) or diverge in conditions from open and closed circuit.

The functioning of our improved algorithm is based on the determination of the electric power panels, detecting its maximum and comparing it to the optimum voltage predetermined by the optimum model of the optimal functioning of the PV panels [10]. In our case, we compare the optimal voltage of V_{optmin} = 12 V and V_{optmax} = 16 V determined by the model of PV panels (Figure 3). As shown in the algorithm in Figure 3, after the calculation of the power derivative, its sign will be known, and then the following structure will be executed:

- The sign of the derivative of power being tested:
  - Positive Derivative: normal state is not going to change anything.
  - Negative derivative: the value of the voltage ($V_{max} > V > V_{min}$) is tested if it is within the range planned:
    - If yes, the timer is tested (TMP)
      - If (TMP = 1) (timer complete): Changing the value of V_{state} (the state of evolution) and resets the timer TMP.
      - Else: no operation.
    - Else: test the location of the tension (V)
      - If ($V < V_{min}$): test of the evolution of V:
        - If ($\Delta V < 0$): V_{state} value is changed.
        - Else: it keeps the same value V_{state}.
      - Else: test of the evolution of V:
        - If ($\Delta V > 0$): Vstate value is changed.
        - Else: it keeps the same value V_{state}.

Then the value V_{state} is tested to increment or decrement the value of the duty cycle.

In addition to improving the efficiency of our system, this algorithm can also treat the divergence problem of the system caused, for example, by a sudden variation in the solar radiation. If the system evolves towards the maximal power point MPP, the algorithm works then as described above. On the other hand, if the system does not evolve towards the MPP, the algorithm will invert the MPP research direction after a passing determined delay, also avoiding problems that may occur during the conversion and the divergence of the system caused by a sudden change of the solar radiation or load variation.

In Figure 4, we have plotted the power-voltage characteristics of the PV generator and the typical results of simulations in ISIS of PWM signal generated by the microcontroller. The two following situations show us how the operating point of the PV converges to the MPP:

- The panel power is increasing when the duty cycle is increasing ($\frac{dP_{PV}}{d\alpha} > 0$) (evolution of A to B).

- The panel power is increasing when the duty cycle is decreasing ($\frac{dP_{PV}}{d\alpha} > 0$) (evolution of C to D).

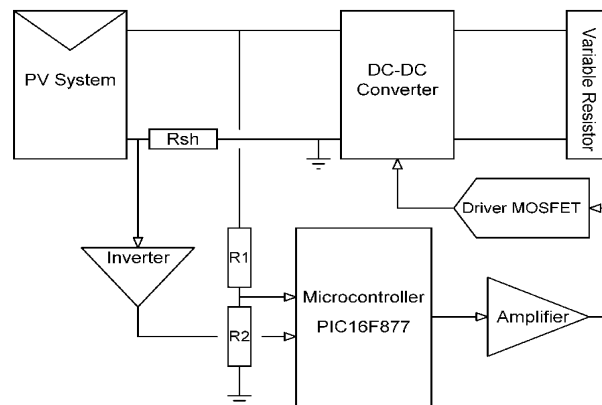**Figure 2.** Block diagram of the digital power point tracking (MPPT) control.

Figure 3. MPPT algorithm and optimal voltage (*V*opt) of the photovoltaic voltage (PV) module depending on the lighting and temperature.
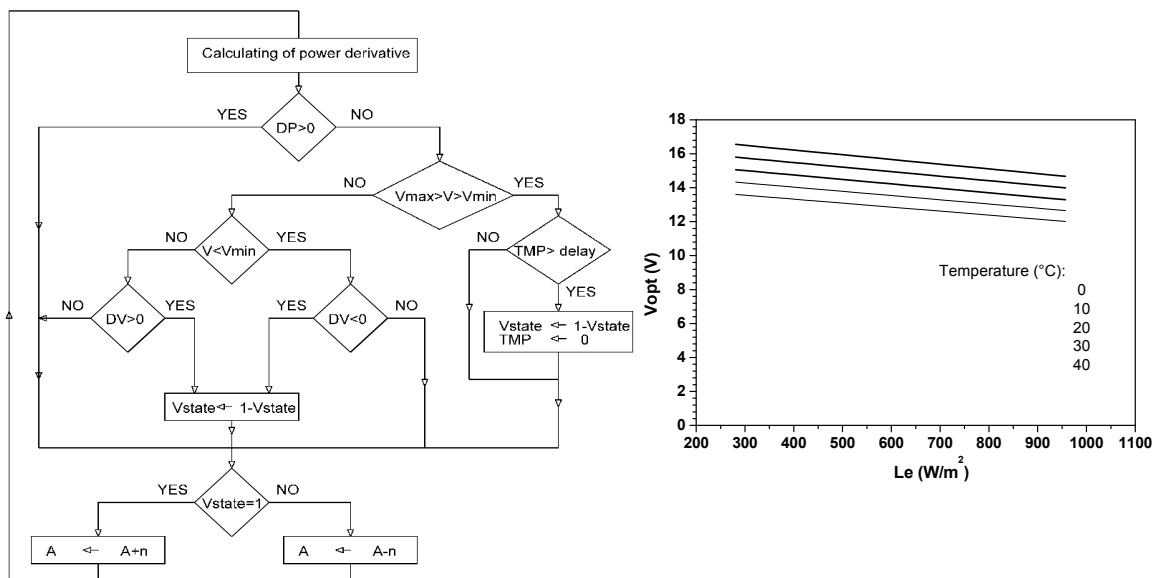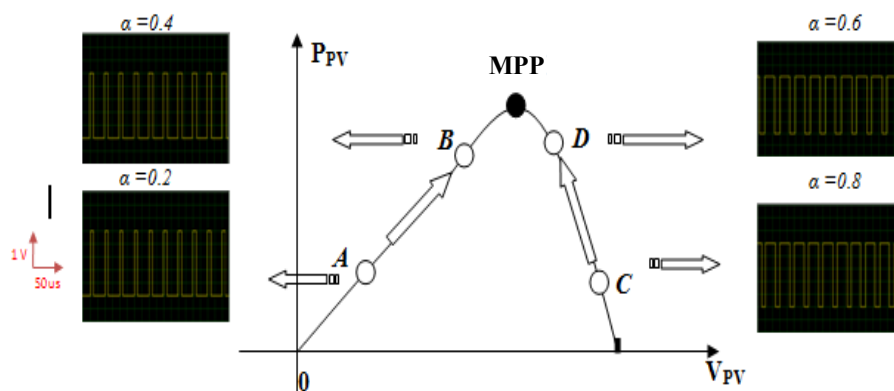
Figure 4. Variations of the simulated PWM signal used to view its influence on the PV panel power.

These results show the good performance and convergence of the PV system equipped with MPPT control (Figure 4) according to the MPP algorithm as illustrated in Figure 3. In Section 3, we analyze the validation of all the results from the PV system designed and implemented in this work.

2.3. Batteries Charge/Discharge Control

The prototype of our realization (Figure 1) carries out the charge/discharge control of batteries in the presence of MPPT control. Therefore, to analyze the techniques of control [15,16], we study in this paper the process charge/discharge when PV panels are connected directly to the batteries (Figure 5) according to two phases of control (Figure 6) [17]: constant current (CC) provided by panels and constant voltage (CV) fixed by the regulator (CV). This enables us to analyze the performances of the technique. The different blocks of the control system are (Figure 5):

- Block of control and acquisition: which consists mainly of a microcontroller (PIC 16F877) to treat the data and controlling the state of charge.
- Block of Power: it is the intermediary between the PV panel and battery, and between battery and load. They are controlled by the block of control.

The process of charge/discharge is performed according to the algorithm presented in Figure 7. It consists of making acquisitions of samples (voltage and current), and calculating their median values. These values, displayed on LCD or computer, are compared to set points (voltage and current) that determine charging and discharging phase of batteries by acting on the power block. To know the state of charge, we used the technique of open circuit voltage (V_{oc}) which lets the battery rest until the stabilization of the voltage V_{bat}, and makes a comparison with tables indicating the state of charge *versus* V_{oc} [18].

To ensure the good performance, in particular, the process charge/discharge of batteries, we have simulated the operation of the system in Figure 5, by taking into account the algorithm in Figure 7, in PROTUES ISIS software [19]. The statement of the typical voltage (V_{bat}) and current (I_{bat}) of battery, during a charge/discharge cycle are represented in Figure 8. It appears an operation that depends on time (t):

- When $t_0 < t < t_2$: during this stage the voltage of battery is between $V_d = 11.8$ V and $V_r = 14.4$ V. Simulation in ISIS shows that when $t < t_1$ the PIC generates two signals: a signal in a low state "0" to ensure the charge of batteries. Another in a high state is "1" to stop the discharge when V_{bat} approach of V_d, or with the state "0" to authorize the discharge when V_{bat} is higher than V_d. This stage is characterized by the increase of V_{bat} voltage, and the battery is charged with the maximum current supplied until $V_{bat} = V_r$. At the end of the process ($t = t_1$), the battery is charged to more than 80%. To improve the charge of the battery and to protect it from the overcharge when $t > t_1$ (Figure 8), the voltage of battery V_{bat} is regulated around V_r (by pulsed currents during increasing time intervals). This shows that the total charge current decreases [13] and the state of charge is greater than 90% (end of charge).

- When $t_2 < t < t_3$: this stage corresponds to the discharge of battery ($V_d < V_{bat} \leq V_r$) and the PIC generates a signal to authorize the discharge $V_{bat} > V_d$. The voltage V_{bat} decreases gradually until $V_{bat} = V_d$ which corresponds to a state of discharge of 80%.

- When $t_3 < t < t_4$: the V_{bat} voltage is slightly lower than V_d, the PIC generates a signal to stop the discharge and to protect the battery against deep discharge, and another signal to authorize the charge.

- When $t > t_4$: another signal charge/discharge is repeated.

The whole results obtained in ISIS shows the good performance of the charge/discharge control and in particular the algorithm in Figure 7.
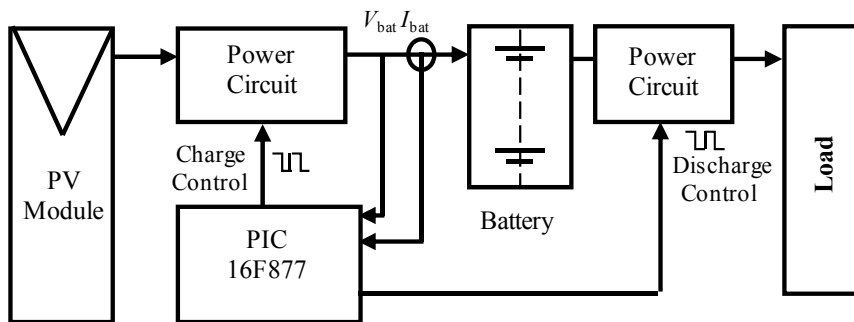
Figure 5. Synoptic diagram of control system.

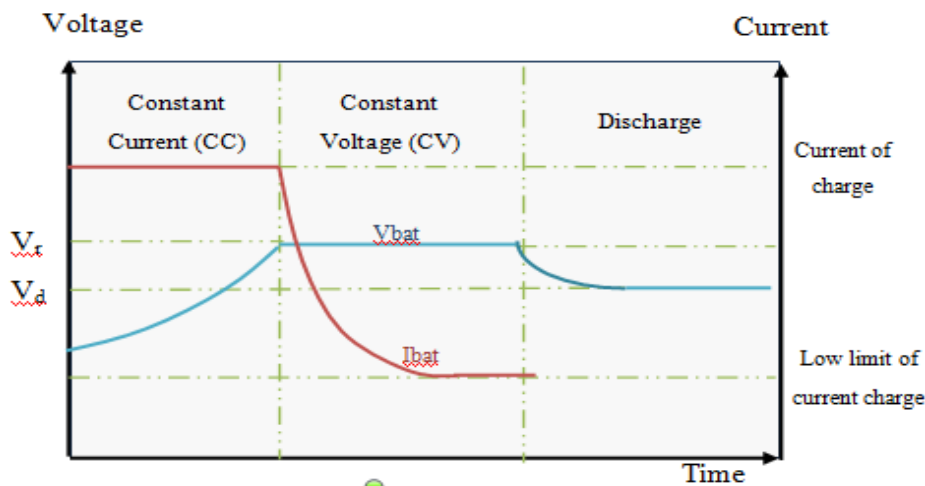**Figure 6.** Control stages (CC/CV) of process charge/discharge.
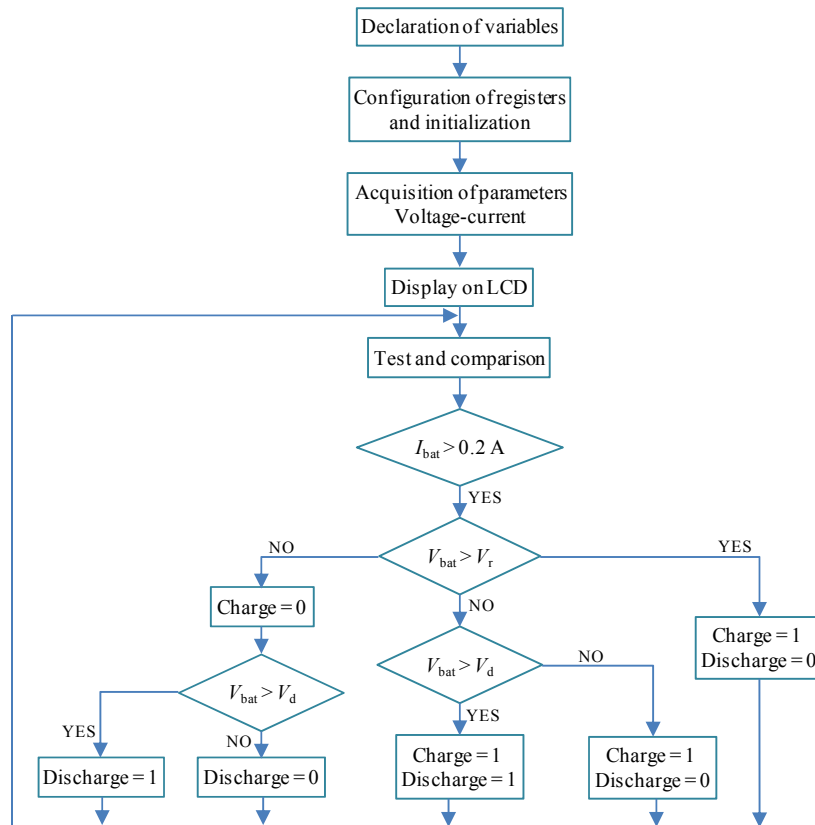
Figure 7. Control algorithm of process charge/discharge.
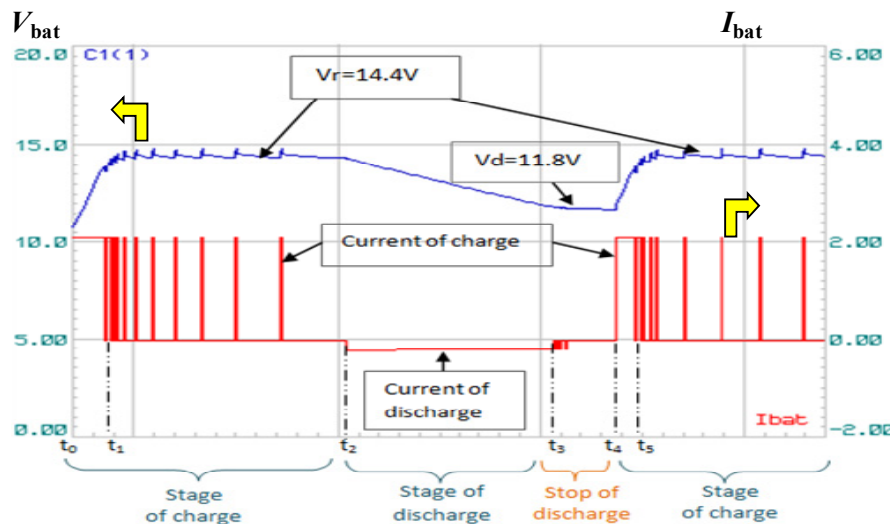

Figure 8. The battery voltage (V_{bat}) and current (I_{bat}) of charge/discharge process.

2.4. Sun Tracking System

2.4.1. Structure and Functioning

To provide a powerful sun tracker and capture the maximum intensity of radiation, we have designed a system that sets the PV panels using the Light Dependent Resistor (LDR) sensors [6]. In this paper, we study the feasibility of the system. The block diagram of the complete system is shown in Figure 9. This system contains:

- Mechanical support for sun tracking which is altazimuth mount and the coordinate system used is the horizontal azimuth [20]. It is composed of two cylinders: the first cylinder performs the vertical rotation and the second performs the horizontal rotation. These two cylinders are associated with DC motors (bearing voltages and currents of the order of 36 V and 4.8 A). Rotation Speed and direction depends on voltages and currents values and signs supplied by the control unit and power.
- An optocoupler that acts as a galvanic insulator between the microcontroller and the power circuit.
- Processing unit, command and control, whose role is to manage the movements of the PV panel. This block is based on using a microcontroller provided with a crystal oscillator frequency of 4 MHz. Its role is to convert the light intensity detected by the four sensors LDR (C1, C2, C3 and C4) from the analog ports RA0, RA1, RA2 and RA3 [6], then sends commands to move the jacks at a certain speed through a double speed control. This is achieved by using the technique of imputing width modulation (PWM) with outputs (PWM1 and PWM2) of PIC 16F877 through a power interface (system L 293B). This interface is formed by two H-bridges that receive commands from the microcontroller through the following pins:

  - ENNABLE 1 and ENNABLE 2 pins receive the signals from the PIC's outputs (PWM1, PWM2), and sends the set point speed.
  - The pins—Input 1, Input 2, Input 3 and Input 4—manage the input rotation on the following order of the microcontroller (Table 1).

The permanent orientation of the PV panel face to the sun is performed by a tracking algorithm (Figure 10). This algorithm is based on the comparison of different illuminations converted into voltages by the PIC. The main steps of this algorithm are:

- Configuring pins for inputs and outputs of the PIC.
- Playback of different voltages (proportional to the illumination) from the four sensors LDR.
- Comparison of the voltages V_1, V_2, V_3, and V_4, converted by the PIC.
- Activating the two next pins RC1and RC2 of PIC to generate two PWM signals and give the proper impetus for the rotation of the two engines in the shown cases (Table 2).The displacement of the PV panel took place whenever the PIC detects a voltage unbalance sensors. In the following situations:

  - $V_1 < V_2$ and $V_3 < V_4$: the PIC generates two duty cycle PWM for each of its two cylinders moving in the positive direction, we activate the pin Input1 and pin Input3 of the circuit L293B.
  - $V_1 > V_2$ and $V_3 > V_4$: the PIC generates two duty cycle PWM for each of its two cylinders moving in the negative direction, we activate the pin Input2 and pine Input4 of the circuit L293B.
  - $V_1 = V_2$ and $V_3 > V_4$: PIC generates a single duty cycle PWM to move a single cylinder in the negative sense, we disable pin Input1and pin Input2 and activate the pin Input4 and pin Input3 of the circuit.
  - $V_1 = V_2$ and $V_3 = V_4$: both cylinders are stopped.

Figure 9. LDR sensor sand mechanical support (**A**), Command and control of the follower of the sun (**B**).
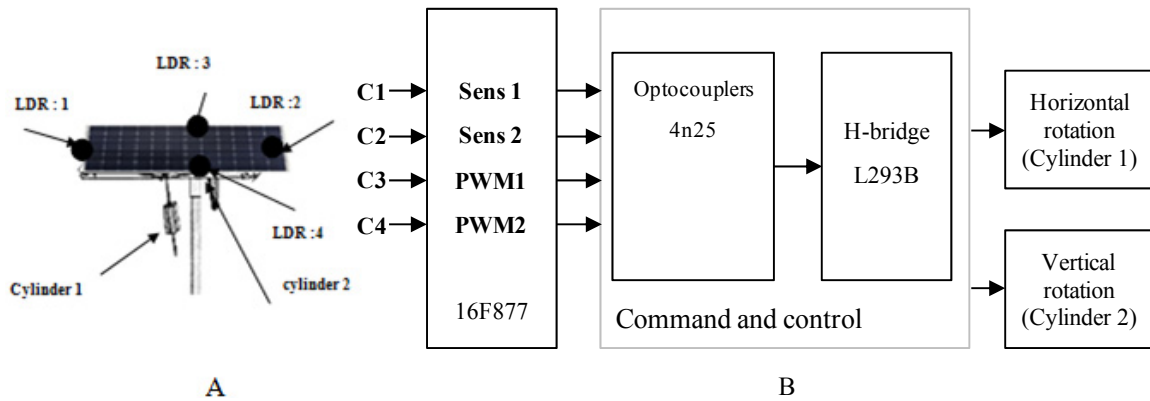

A
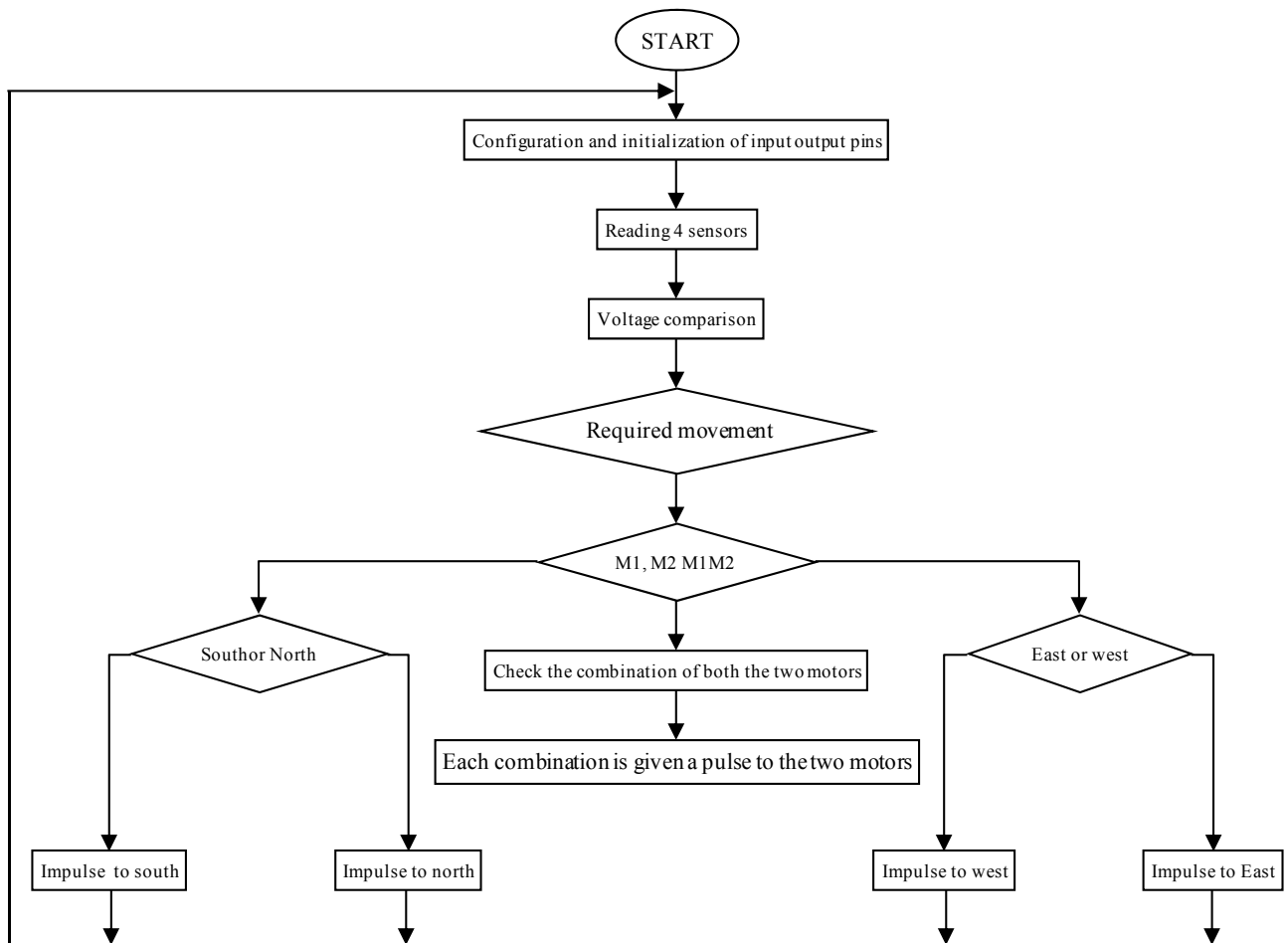
B

Figure 10. Algorithm of the sun using LDR sensors.

Table 1. Table of different sequences.

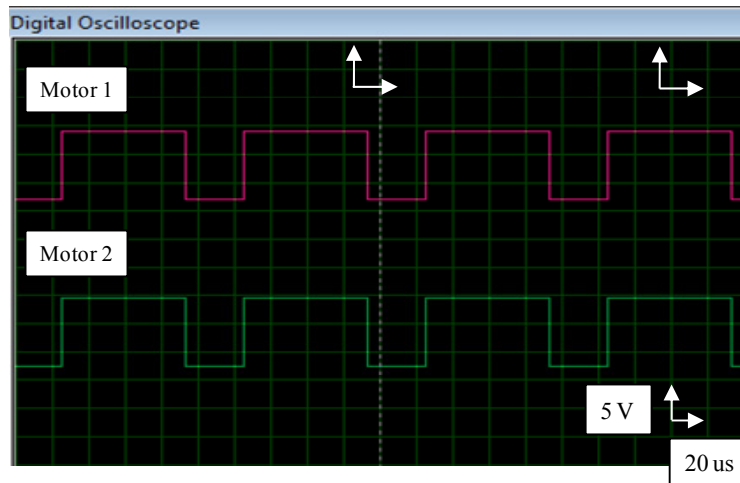| Motor 1			Motor 2		
Input 1	Input 2	State motor 1	Input 3	Input 4	State motor 2
0	0	Stopping the motor	0	0	Stopping the motor
0	1	Sens 1	0	1	Sens 1
1	0	Sens 2	1	0	Sens 2
1	1	Stopping the motor	1	1	Stopping the motor

Table 2. Positions of the solar panel by the imbalance of voltages (V_1, V_2, V_3 and V_4) of the sensors LDR.

Imbalance of voltages	$V_3 < V_4$	$V_3 > V_4$	$V_3 = V_4$
$V_1 < V_2$	Oriented panel: • East to West • South to North	Oriented panel: • East to West • North to South	Oriented panel: • East to West
$V_1 > V_2$	Oriented panel: • West to East • South to North	Oriented panel: • West to East • North to South	Oriented panel: • West to East
$V_1 = V_2$	Oriented panel: • South to North	Oriented panel: • North to South	Stopping the engine

2.4.2. Simulation Results

We have analyzed the operation of the electronic circuit of the sun tracking system in the software simulation of electronic circuits and programmable devices Proteus ISIS, and we identified the different electrical parameters (voltage and current) system for a given position ($V_1 < V_2$, $V_3 > V_4$). Typical results obtained in Figures 11 and 12 show:

- By varying the illumination by the associated sensors LDR potentiometer, we fix the situation:
  - $V_1 = 0.06$ V for illumination equal to 1000 W/m^2,
  - $V_2 = 0.11$ V for illumination equal to765 W/m^2,
  - $V_3 = 0.19$ V for illumination equal to 470 W/m^2,
  - $V_4 = 0.14$ V for illumination equal to 649 W/m^2.

- After conversion of different illuminations, the PIC 16F877 generates two frequencies of 10 kHz and a duty cycle of 0.75 PWM signal (Figure 11). These signals provide a rotational speed of the two motors.

- The power circuit L293B receives commands from the PIC 16F877 to move motor 1 in the direction "Forward" (positive current) and motor 2 in the direction "Backward" (negative current) (Figure 12).

- When the PV panel receives the maximum intensity, voltage sensors are virtually identical and communication with the engine stops (absence of PWM and current signals).

Figure 11. Terminal signals of the motor1 and motor 2.

Figure 12. Variation of the current of motor 1and motor 2.
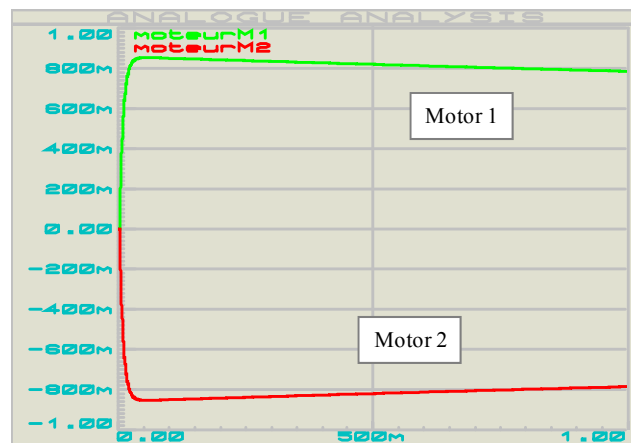
3. Experimental Results

3.1. Experimental Procedure

The subsystems and the PV system (PV panel "SP75", MPPT control, charges/discharge, sun tracking), which were the object of our study are displayed on Figure 13. In this PV system:

- The DC-DC Boost converter works in its continuous regime at the operating frequency of 10 kHz. The microcontroller must generate a square signal, with amplitude of 10 volts and a variable duty cycle according to the digital MPPT algorithm.
- Charges/discharge: is formed by a command which plays the role of a regulator charges/discharge, and solar battery (12 V, 110 Ah).
- Sun tracking: This system is composed by a follower carried for movement in two axes from a system monitoring and control.

Figure 13. Experimental procedure, (**a**) MPPT control; (**b**) charges/discharge; (**c**) sun tracking.

| (a) | (b) | (c) |

3.2. Digital MPPT Contol

To validate the functioning of the system on Figure 2, we tested the PV system designed in this work (Figure 13) according to the load with and without MPPT control (Figure 14). In Figure 14, we also represented the experimental and the optimal simulated results obtained by PSPICE simulator [1,2]). We deduce that, without the MPPT control, the power supplied by the PV panels is much lower than that which is optimal. We also deduce that we have a perfect match between the optimal simulated electric quantities (voltage, current and power) and experimental ones using the MPPT control, which shows the smooth running of the MPPT control.

To validate the performances of the photovoltaic systems, we followed their functioning during a whole day presenting sudden changes in light intensity. In Figure 15, we represented the variation of the illumination, the experimental results (with and without Digital MPPT Control) and the optimal simulated results of the PV panel power (P_{PV}). Also in Figure 15, we represented powers losses supplied by PV panels. These results show:

- By using the MPPT control, we have a good concordance between the optimal simulated results and the experimental ones, with very low power losses "less than 5%"
- Using the PV system without the MPPT control, the power losses can reach 80%

- The PV system works in optimal conditions throughout the day. At every perturbation of the system (sudden variations in illumination, presence of other MPPs, *etc.*) it detects the perturbation (dysfunction, wrong MPP, *etc.*) and ensures optimum functioning and the stability of the PV system.

Figure 14. Electric quantities (voltage (**a**), current (**b**), power (**c**)) of the PV panel (Experimental and optimal simulated with Pspice) by modifying resistor values with and without Digital MPPT Control.

(**a**)

(**b**)

(**c**)
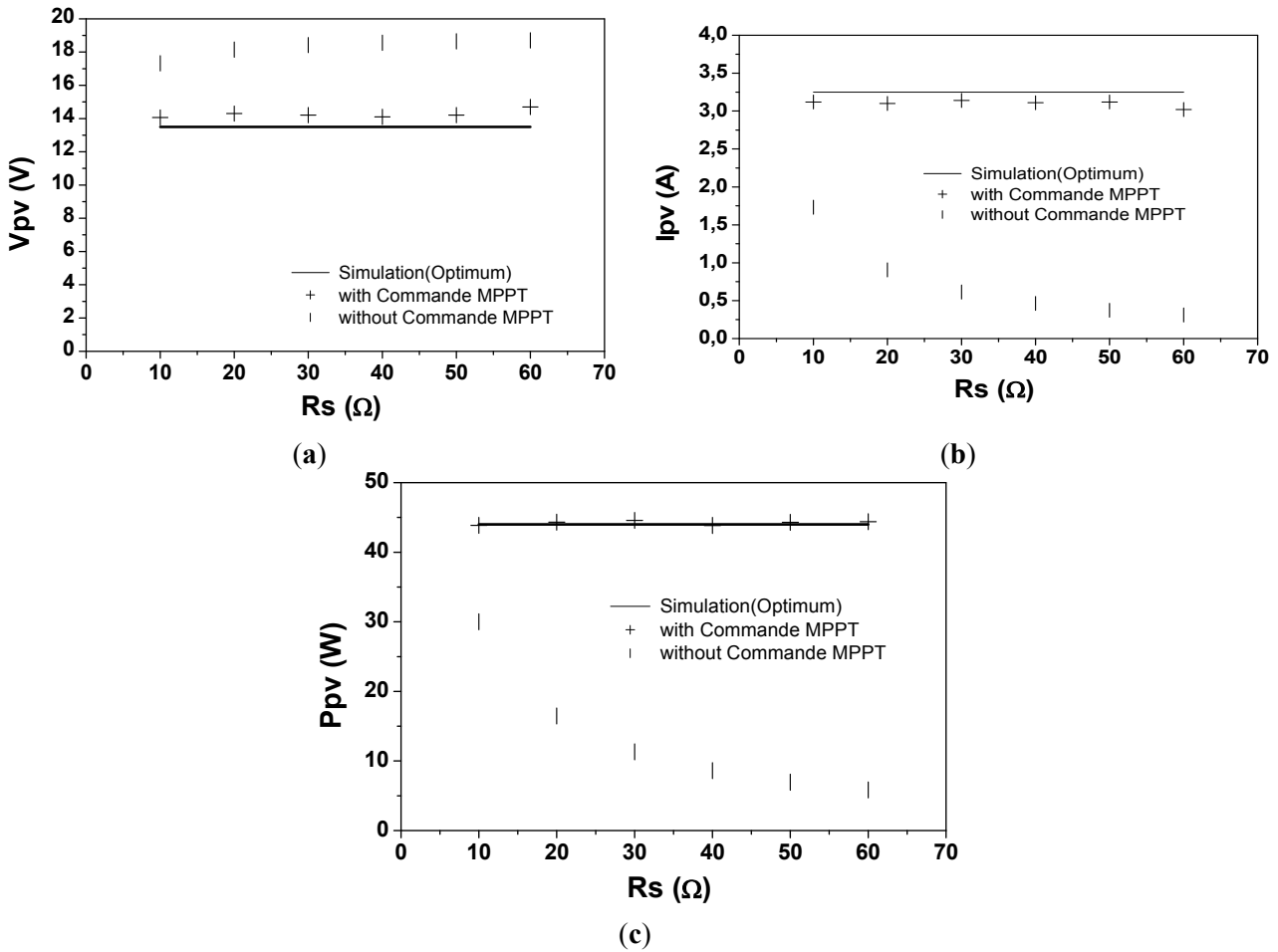
Figure 15. Illumination (Le) (**a**), power (**b**) of a PV panel (experimental and simulated (optimum)) and power losses (**c**) for a day, with and without Digital MPPT control.

(**a**)

(**b**)

Figure 15. *Cont.*

(c)
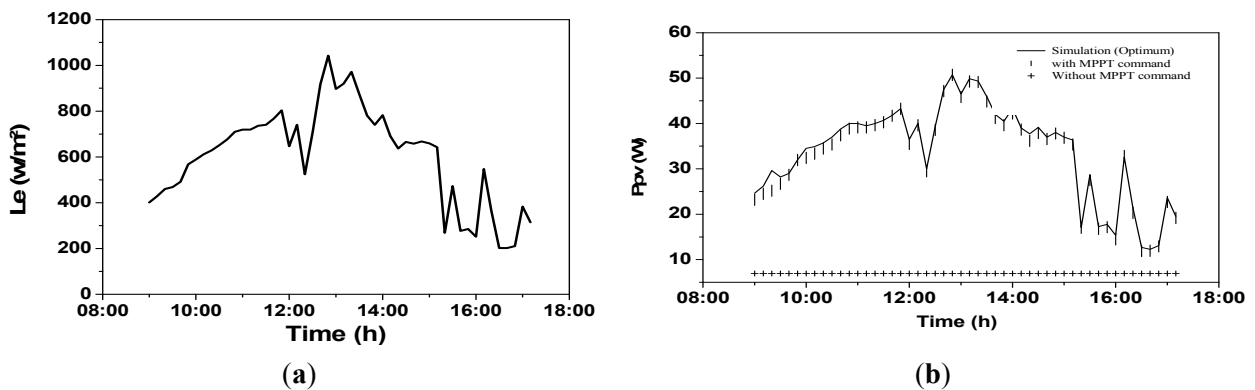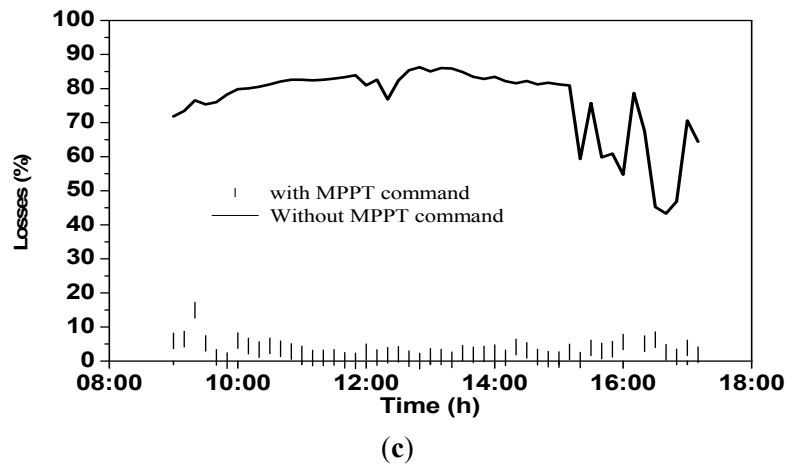
3.3. Batteries Charge/Discharge Control

In the typical experimentation of the controller of charge-discharge (Figure 13b) during whole days, where the charging current did not exceed 3 A, there was the ability to raise the voltage and charge current (Figure 16) and the state of charge of battery (Figure 17). The results of the discharge will be presented in other works. It appears at the beginning of the charge (lower than 900 min), the voltage V_{bat} increases and the charge current is practically constant (I_{bat} = 3 A). Once the voltage V_{bat} reaches V_r = 14.4 V, the voltage Vbat is constant and the charge current decreases gradually. The fluctuations of the current and the voltage, or the reductions in the current during time interval 600 mn and 900 mn, are caused by the abrupt variations of illumination during the day. From the measurement of the voltage $V_{bat} = V_{oc}$ at rest, we have estimated the charging rate of battery. As shown in Figure 16, when it reaches the voltage V_r = 14.4 V, the battery is charged to 80% and after the application of the impulses of current the state of charge reaches 92%. All these results show the good performance of the stage of charge and especially the control by the microcontroller. Note that during this charging process, the PV panels are connected directly to the battery (Figure 13). The statement of the power and power losses by the panels (Figure 18), compared to their MPP, shows that losses can reach 30% in the first stage of charge (constant current). To exploit the maximum power of panels and reduce the charging time of the batteries, we associate the system charge/discharge control to the MPPT control. The results will be presented in other works.

3.4. Sun Tracking System

To validate the simulation results obtained in this section, we tested the function of each system block. Typical results obtained in Figures 19–23 show:

- During the day, the illumination intensity maximum is of the order of 1000 W/m^2 (Figure 19). During this day, the terminal voltage decreases with a LDR sensor illumination (Figure 20). Figure 20 also shows the results obtained in Proteus ISIS. We deduce a very good agreement between experiment and simulation, and thus validating responses LDR sensors in Proteus ISIS.
- For a similar simulated conditions in Proteus ISIS (V_1 = 0.8 V, V_2 = 1.32 V, V_3 = 2.71 V, V_4 = 1.02 V). Controlling the speed of the two motors is enabled by two PWM signals generated

by the PIC 16F877 a frequency of about 10 kHz, and a duty cycle α of 0.75 (Figure 21). The PIC generates signals to reach the equilibrium position (collection of maximum illumination): forward rotation of the motor 1 by a positive current, and a backward rotation of the motor 2 by a negative current (Figure 22).

- The optimal position of the PV panel is obtained when a balance of tension sensor LDR ($V_1 = V_2 = 0.7$ V, and $V_3 = V_4 = 1.51$ V). Both engines are off and L293B circuit generates no current (Figure 23).

The comparison of these experimental results to those obtained in ISIS shows a very good concordance between experiment and simulation, on the one hand, and the proper functioning of tracking the sun, on the other. The control unit generates signals to activate the motor (speed and direction of rotation) and properly orient the PV panel to capture the maximum of the intensity of the illumination.

All the obtained results show the feasibility of a tracking system of two-axis, with no electric energy consumption (24 W), keeping the surface of the solar panels perpendicular to sun light permanently and a simple automatic control.

Figure 16. Current and voltage of charge of the battery (12 V, 110 Ah).
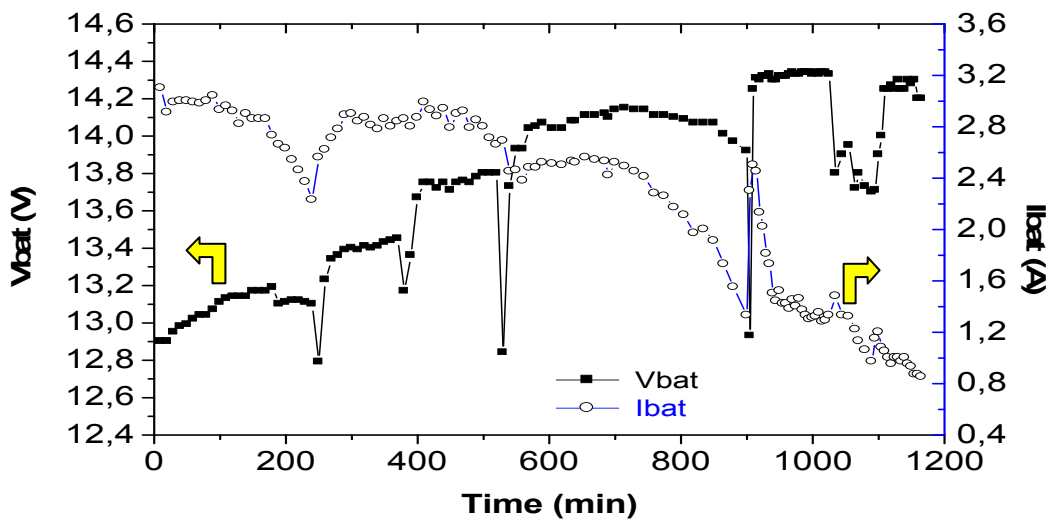
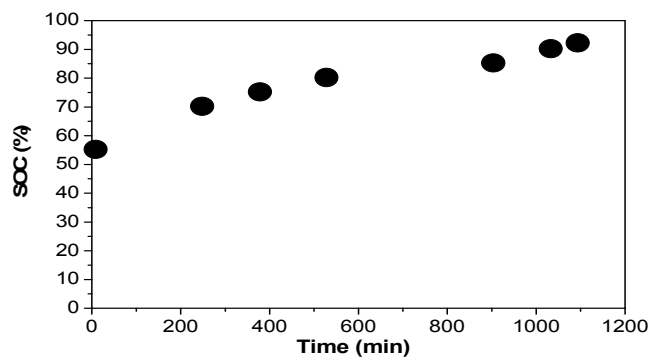**Figure 17.** State of charge (SOC) of battery.

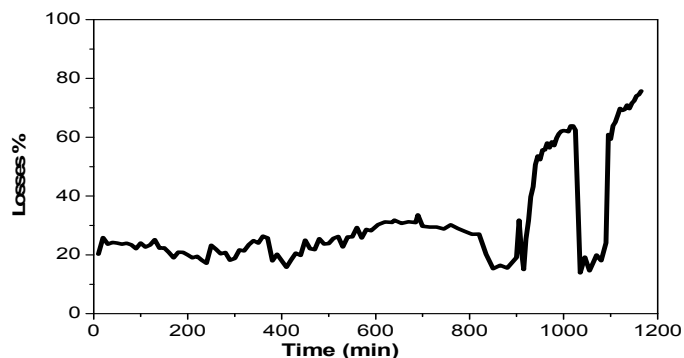**Figure 18.** Losses of power of PV panel during the charge of the battery.

Figure 19. Variation of illumination with time.
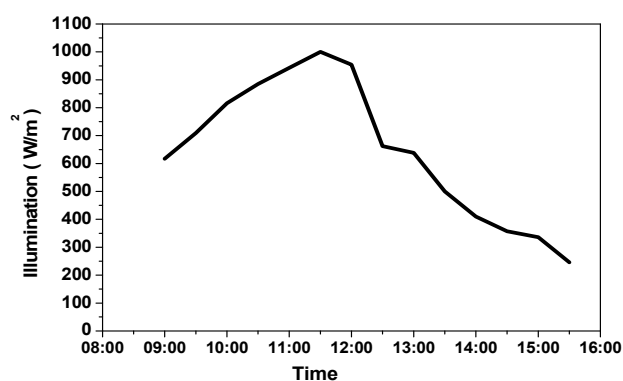

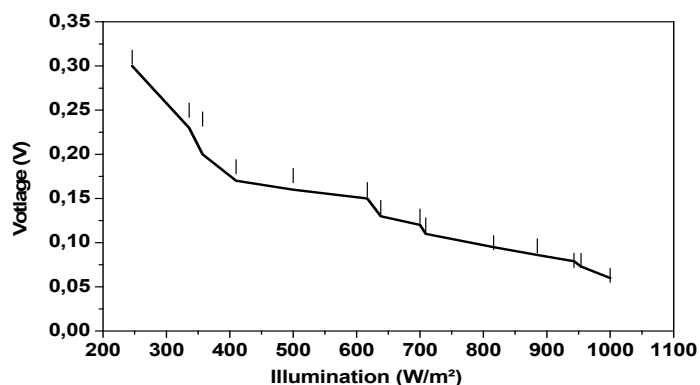**Figure 20.** Variation of the sensor LDR voltage in function of illumination.

Figure 21. Generating PWM signals by PIC for controlling the rotational speed of the two motors for α = 0.75. (Scales: 2 V/Div, 20 μs/Div).
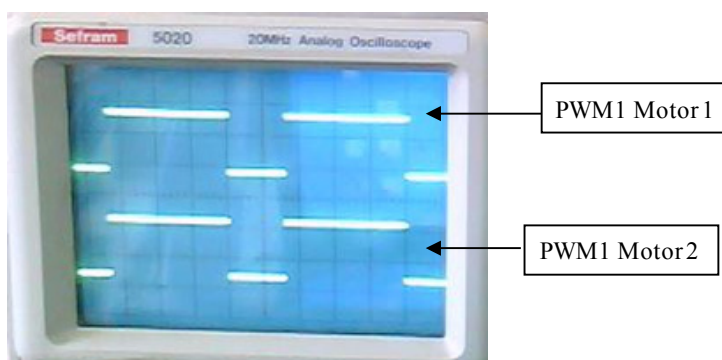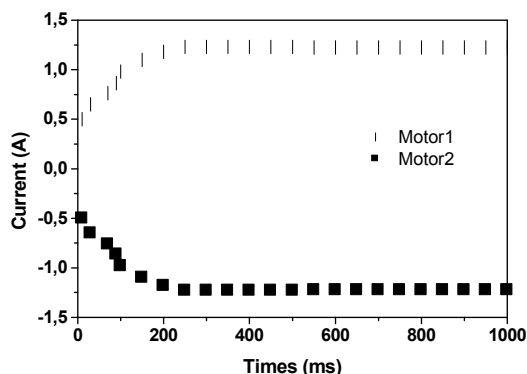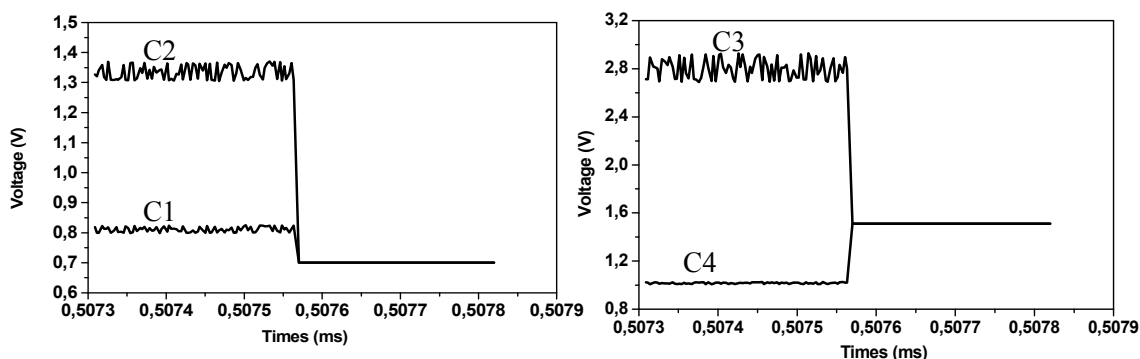
Figure 22. Current variation of motor1 and motor 2.

Figure 23. Voltage variation of the LDR sensor C1, C2, C3 and C4.

4. Conclusions

In this paper, we have studied the design, the realization and the operation of a photovoltaic system performing different tasks: acquisition and supervision, MPPT control, controller of charge/discharge batteries and solar tracking. The results obtained show:

- The good performance of each block of the system using the different modules of the microcontroller "PIC 16F877", such as CAN, PWM and USART modules, to manage different functions (MPPT control, controller of charge/discharge batteries and solar tracking).
- The MPPT control present the improved response time and accuracy of the MPP research, good control independently of the perturbations (Sudden variations of the illumination and the load, *etc.*).
- The controller charge/discharge ensures the control process and monitor the state of charge of the battery lead-acid type rated voltage of 12 V, while exploiting the energy provided by PV panels. This is provided by a microcontroller that performs all functions: acquisition, supervision, regulation, *etc.* The results obtained during the days of experimentation showed the robustness of the PV system (stability, good operating system, good control of charge/discharge batteries and protection against overloading and deep discharge).
- The sun tracking system detects the PV panels to capture the maximum illumination. The mechanical aspect of a solar tracking system, where the focus was on mechanical drive low power option, which allows a possible energy autonomy of the system, and exploitation of solar energy efficiently not only during day light hours, but also scattered light throughout the year.

Acknowledgments

Conflict of Interest

The authors declare no conflict of interest.

References

1. Stéphane, P. Nouvelles architectures distribuées de gestion et de conversion de l'énergie pour les applications photovoltaïques (in French). Doctorat Thesis, de l'Université de Toulouse, Toulouse, France, January 2009.
2. Yaden, M.F.; El Ouariachi, M.; Mrabti, T.; Kassmi, Ka.; Chadli, E.L.; Kassmi, K. Design and Realization of a Photovoltaic System Equipped with a Digital MPPT Control. In Proceedings of the 2nd International Conference on Multimedia Computing and Systems ICMCS'11, Ouarzazate, Morocco, 7–9 April 2011; pp. 1–6.
3. Nicola, F.; Petrone, G. Optimization of perturb and observe maximum power point tracking method. *IEEE Trans. Power Electron.* **2005**, *20*, 963–973.
4. Mrabti, T.; El Ouariachi, M.; Malek, R.; Kassmi, Ka.; Bagui, F.; Olivié, F.; Kassmi, K. Design, realization and optimization of a photovoltaic system equipped with analog maximum power point tracking (MPPT) command and detection circuit of the dysfunction and convergence the system (CDCS). *Int. J. Phys. Sci.* **2011**, *6*, 7865–7888.
5. Karoui, F. Optimisation de stratégies de gestion des batteries au plomb utilisées dans les systèmes photovoltaïques (in French). Ph.D. Thesis, National Institute of Polytechnic, Grenoble, France, 26 October 2007.
6. Mousazadeh, H.; Keyhani, A.; Javadi, A.; Mobli, H.; Abrinia, K.; Sharifi, A. A review of principle and sun-tracking methods for maximizing solar systems output. *Renew. Sustain. Energy Rev.* **2009**, *13*, 1800–1818.
7. Alboteanu, L.; Manolea, G.; Ravigan, F. Positioning Systems for Solar Panels Placed in Isolated Areas. Annals of the University of Craiova, Electrical Engineering Series; University of Craiova, Craiova, Romania, 2006; 30; pp. 163–168.
8. Koutroulis, E.; Klaitzakis, K.; Voulgaris, N. Development of a microcontroller-based photovoltaic maximum power point tracking control system. *IEEE Trans. Power Electron.* **2001**, *16*, 46–54.
9. El Ouariachi, M.; Mrabti, T.; Yaden, M.F.; Kassmi, Ka.; Chadli, El.; Bagui, F.; Kassmi, K. Design and realization of a photovoltaic system equipped with the analogical and digital MPPT command for better exploitation of solar energy. *J. Mater. Environ. Sci.* **2011**, *2*, 538–543.

10. Mrabti, T.; El Ouariachi, M.; Yaden, M.F.; Kassmi, Ka.; Kassmi, K. Characterization and modeling of the electrical performance of the photovoltaic panels and systems. *J. Elect. Eng. Theory Appl.* **2010**, *1*, 100–110.

11. Ramabadran, R.; Mathur, B.L. Effect of shading on series and parallel connected solar pv modules. *Mod. Appl. Sci.* **2009**, *3*, No. 10.

12. Bishop, J.W. Computer simulation of the effects of electrical mismatches in photovoltaic cell interconnection circuits. *Sol. Cells* **1988**, *25*, 73–89.

13. Liu, F.; Kang, Y.; Zhang, Y.; Duan, S. Comparison of P&O and Hill Climbing MPPT Methods for Grid-Connected PV Converter. In Proceedings of the 3rd IEEE Conference on Industrial Electronics and Applications, Singapore, 3–5 June, 2008; pp. 804–807.

14. Boitier,V.; Maussion, P.; Cabal, C. Recherche du maximum de puissance sur les générateurs photovoltaïques (in French). *Enseign. Electrotech. Electron. Ind.* **2008**, *65*, 90–96.

15. The world of accumulators & rechargeable batteries. Available online: http://www.ni-cd.net/accusphp/theorie/plomb/charge.php (accessed on 8 July 2013).

16. Solar energy and photovoltaic electricity. Available online: http://www.cipcsp.com (accessed on 8 July 2013).

17. Emmanuel Patrick, F.V. Production de l'énergie photovoltaïque à la société Nova Diffusion (in French). Master's Thesis, Ngaoundere University, Dang, Cameroun, 2008.

18. James, L.; John, L. *Electric Vehicle Technology Explained*; John Wiley & Sons Ltd.: Chichester, England, 2003.

19. PROTEUS Homepage. Available online: http://www.labcenter.com/index.cfm (accessed on 8 July 2013).

20. Bingöl, O.; Altintaş, A.; Öner, Y. Microcontroller based solar-tracking system and its implementation. *J. Eng. Sci.* **2006**, *12*, 243–248.